Clays and Clay Minerals, Vol. 52, No. 2, 158–170, 2004.

ACOUSTIC AND ELECTROACOUSTIC CHARACTERIZATION OF VARIABLE-CHARGE MINERAL SUSPENSIONS

MARIANNE GUERIN[1], JOHN C. SEAMAN[1,*], CHARLOTTE LEHMANN[1] AND ARTHUR JURGENSON[2]

[1] The University of Georgia, Savannah River Ecology Laboratory, Savannah River Site, Aiken, South Carolina 29802, USA
[2] Savannah River Technology Center, Savannah River Site, Aiken, South Carolina 29802, USA

Abstract—Acoustic and electroacoustic measurements of particle-size distribution (PSD) and zeta potential (ζ potential), respectively, were used to obtain *in situ* measures of the effects of suspension concentration and pH on interactions between mixed-charge clays and clay minerals from a highly weathered sediment. Measurements were obtained in concentrated suspensions as a function of weight fraction and as a function of pH during titrations. Standard dispersion and centrifugation methods were used to obtain a comparative measure of PSD. Thermogravimetric analysis and X-ray diffraction patterns were used to obtain semi-quantitative and descriptive analyses, respectively, of the sediment, which is composed of Fe oxide minerals, kaolinite, gibbsite, quartz, crandallite, chlorite and traces of other clay minerals. Acoustic measurements showed that the PSD of the clay fraction varied with suspension concentration, and electroacoustic measurements showed the 'bulk' ζ potential increased in absolute value as the suspension concentration decreased. Titration results were also sensitive to suspension concentration. Acoustic measurements indicated that the suspensions became unstable at ~pH 7.5−8.0, as the attenuation spectra changed character near this pH and the calculated PSD shifted to a larger particle size. This pH value is near the points of zero charge of goethite and gibbsite, as verified by titrations on mineral standards. The results confirm the central role oxide minerals play in regulating clay mineral interactions in highly weathered sediments, and indicate that the average ζ potential of a suspension may be a poor indicator of controls on suspension stability.

Key Words—Acoustic Spectroscopy, Electroacoustic Spectroscopy, Particle-size Distribution, PSD, Thermogravimetric Analysis, Variable-charge Minerals, Zeta Potential.

INTRODUCTION

Three important characteristics regulating interactions in clay mineral suspensions are: mineralogy, particle-size distribution (PSD) and ζ potential, the potential at the shear plane of the electric double layer (Hunter, 1981, 2001). Particle size and surface charge of clay minerals are important in sorption mechanisms and in transport properties of mineral colloids and associated contaminants, such as heavy metals, through porous media (Bertsch and Seaman, 1999; Seaman *et al*., 1995a, 1995b). The fate of contaminants is frequently tied to that of the colloidal particles coating the coarser fractions of sediments (Bertsch and Seaman, 1999). Fluctuations in groundwater chemistry can remobilize contaminants by detachment of the mineral colloids, or simply by desorption (Bertsch and Seaman, 1999; Ryan and Gschwend, 1994a, 1994b). The effects of suspension concentration, *i.e*. soil/solution ratio and pH on PSD and colloid interactions are particularly important in understanding contaminant remobilization in soils and sediments (Roy *et al*., 1991). The ubiquity and large reactive surface area of Fe oxides give them a central role in controlling solution chemistry and clay mineral interactions (Bertsch and Seaman, 1999; Bunn, 2002; Cerpa *et al*., 1999; Seaman *et al*., 1997).

* E-mail address of corresponding author:
seaman@srel.edu
DOI: 10.1346/CCMN.2004.0520202

In mixed-charge sediments, constant-charge clay minerals (aluminosilicates with a permanent structural charge) interact with oxide minerals of Fe and Al, which are negatively and positively charged, respectively, at the normal pH of groundwater. Iron oxides or oxyhydroxides are known to form close associations with clay minerals, forming discontinuous layers or small aggregates on the negatively charged surfaces of clays (Bertsch and Seaman, 1999; Bunn, 2002; Hong and Xiao-Nian, 1992; Seaman *et al*., 1997). Some studies have suggested that the 'binding agents' providing physical stability in soils are mainly poorly crystalline or amorphous phases of Fe, Si or Al (Arias *et al*., 1995; Swartz *et al*., 1997), and that crystalline phases are more likely to form discrete aggregates. Transmission electron microscopy (TEM) images have shown that both amorphous and crystalline Fe oxides are associated with clay components in soils (Bertsch and Seaman, 1999; Seaman *et al*., 1997; Swartz *et al*., 1997). In addition, some researchers have determined that Al and Fe oxides may behave either as flocculants or as dispersants in mixtures of variable charge-constant charge mineral colloids, depending on the relative concentrations (Arias *et al*., 1995). The surface chemistry of variable-charge mineral assemblages are thus characterized by complex physicochemical interactions between the individual components (Bertsch and Seaman, 1999). These, and other findings (Anderson and Benjamin, 1990; Arias *et al*., 1995; Honeyman,

1984; Yong and Ohtsubo, 1987), indicate that the behavior of clay mineral assemblages is not simply the sum of individual mineral characteristics.

Recently, significant advances have been made in the theory and application of acoustic and electroacoustic spectroscopies to characterize PSD and ζ potential of concentrated suspensions (Dukhin and Goetz, 1996b, 1998, 2000; Dukhin *et al*., 1999a, 1999b, 2001; Hunter, 1998, 2001; O'Brien *et al*., 1995). Acoustic attenuation spectra can be utilized to give a measure of the PSD, while electroacoustic measurements give a measure of ζ potential. These spectroscopies extend or replace other techniques, particularly in concentrated suspensions where optical techniques fail due to the requirement of extreme dilution and suspension stability.

With few exceptions, the use of acoustics and electroacoustics has been confined mainly to industrial applications (Galassi *et al*., 2001; Johnson *et al*., 1998) or the study of single clay minerals (Costa *et al*., 1999; Hunter and James, 1992; Johnson *et al*., 1999a, 1999b; Rowlands and Hunter, 1992; Sindi *et al*., 1996), despite the clear potential for the technique to characterize environmentally significant clay mineral suspensions. Techniques such as SEM and TEM have an extremely important role to play in particle sizing, especially for determining particle shape, that neither acoustics nor light scattering can replace (Hunter, 2001). However, acoustic techniques have the important advantage that *in situ* concurrent measurements of particle size and ζ potential can be made, and thus are not subject to changes in particle-particle interactions due to dilution, to drying, or to pH adjustments to obtain suspension dispersion in fractionation methods (Hunter, 2001; Jackson, 1979). Acoustic and electroacoustic spectroscopies are applicable in either relatively dilute or concentrated suspensions, and can accommodate a large range of particle sizes (Dukhin and Goetz, 1996a; Hunter, 2001). The reader is referred to reviews of acoustic and electroacoustic spectroscopies for further details on these techniques (Dukhin and Goetz, 1996a, 2002; Dukhin *et al*., 1999a; Hunter, 1998, 2001; McClements, 1991) (see also Guerin and Seaman (2004), this issue).

The objective of the current study is to characterize the effects of suspension concentration and pH on interactions between the clay and clay mineral constituents found in a highly weathered, variable-charge sediment from the Atlantic Coastal Plain region of the South Eastern USA (Seaman *et al*., 1995b), the 'Tobacco Road' (TR) sediment. The main analytical method consists of the combined use of acoustic and electroacoustic spectroscopies to characterize the *in situ* PSD and ζ potential of concentrated suspensions in response to changes in solution characteristics. The motivation is to improve the understanding of suspension concentration effects on the colloidal interactions as a part of separate contaminant transport studies. In addition to acoustic techniques, we obtain independent measurements of PSD using fractionation by dispersion and centrifugation. Mineralogy is characterized semi-quantitatively using thermogravimetric analysis (TGA). X-ray diffraction (XRD) patterns are used to confirm and extend results from other measurement techniques in assessing mineralogy and particle interactions.

EXPERIMENTAL

Materials

Tobacco Road (TR) is a generic name for a highly weathered, low-pH, low-ionic strength, low-CEC, organic-poor sediment horizon found in the Barnwell aquifer at the Savannah River Site, near Aiken, South Carolina (Seaman *et al*., 1995a, 1995b; Strom and Kaback, 1992). The mineralogy (Table 1) consists of Fe-bearing minerals such as goethite and hematite (referred to as 'Fe oxides' in this paper), as well as gibbsite, quartz, kaolinite, chlorite/vermiculite, illite and crandallite. An artificial groundwater (AGW) solution was used in suspensions to approximate the natural soil solution composition (Seaman *et al*., 1995a, 1995b; Strom and Kaback, 1992). Artificial groundwater is a low-ionic strength, low-pH solution (Table 1, footnote #3). The dry sediment was sieved to 2 mm, and rewet in AGW from an air-dried state. Suspensions prepared for further analysis were composed of the clay fraction, combined with the silt fraction in some suspensions.

Single mineral samples used for comparison consisted of kaolin (KGa-1, Purdue University, Source Clay Minerals Repository), goethite prepared as described in Schwertmann and Cornell (1991), and gibbsite (ALCOA #H-710-B). Ottawa sand (20-30 mesh standard) was crushed in a Mixer-Mill using agate containers and balls, and heated to 550ºC for 48 h to remove organic contaminants. The KGa-1 kaolin was dispersed with NaCl, and fractionated via centrifugation to obtain a <2 μm fraction. The crushed Ottawa sand was fractionated at ~20 μm by settling and decantation in Milli-Q water. The gibbsite mean particle size was specified as 1.0 μm, as determined by Sedigraph; the goethite particle size expected using this synthesis method was >0.3 μm. Mineral standard suspensions for acoustic analysis were dialyzed in a concentrated AGW solution (~0.2 moles L^{-1}) for ~48 h, followed by dialysis at the final solution concentration for at least 2 days. The goethite suspension was dialyzed for an extended period as previous work indicated that this may alleviate problems with air bubbles in the suspensions.

Methods

Two types of experiments were performed on TR Air-Dried (TRAD) suspensions at different suspension concentrations, a dilution experiment with TRAD #1, and titration experiments with TRAD #2. Both sets of suspensions (Table 2) were prepared by agitating

Table 1. Characterization of the TRAD sediment (sieved to 2.0 mm).

	Description	Quantity
Mineralogy*		
	Major components[1]	Q, Ka, Gi, G
	Minor/trace[2]	He, Cr, Il, Chl, Ru, An,O
pH		
	Sediment in Milli-Q	5.2
	Sediment in AGW[3]	5.4
	'Middle' #1[4] in AGW	4.7−5.1
	'Middle' #2[5] in AGW	4.6−4.9
	'Bottom' fraction #1 in AGW	~4.5
Sieving, dispersion sizing		
>v. fine sand	70−2000 μm	91%
med. silt−v. fine sand	20−70 μm	3%
fine−med. silt	2−20 μm	3%
clay	<2 μm	3%

* Q = quartz, Ka = kaolinite, G = Fe oxides/goethite, Gi = gibbsite, He = hematite, Cr = crandallite, Il = illite, Chl = chlorite, Ru = rutile, An = anatase, O = other
[1] See Table 4 and Figure 1 for related information
[2] Relative quantities unknown
[3] AGW characteristics: pH ≈ 5.0; $[Cl^-]$ ≈ 0.14 mM; $[SO_4^{2-}]$ <0.01 mM; $[Na^+]$ ≈ 0.06 mM; $[K^+]$ <0.01 mM; $[Ca^{2+}]$, $[Mg^{2+}]$ ≈ 0.02 mM; mM ≈ 10^{-3} moles L^{-1}
[4] See Table 2, 3−24 wt.% samples. Enriched in quartz, contains larger particles
[5] See Table 2, 2.5 and 5.0 wt.% samples

~50−100 g of sediment in AGW in 250 mL Nalgene containers. The sediment separated into three distinct layers with agitation and subsequent settling. Sedimentation time was determined by the appearance of the distinct layers. The 'top' fraction consisted of suspended colloidal particles, the 'middle' fraction, a thick reddish-yellow suspension, was evident via a clear color demarcation, and the 'bottom' fraction consisted of larger quartz particles. The middle and top sections appeared to contain minerals with Fe-oxide 'coatings' as evidenced by the reddish-yellow color and subsequently verified by TGA. The top and middle fractions were pipetted off for further acoustic/electroacoustic characterization, leaving a coarse, compacted sandy (quartz) layer. Weight fractions were calculated using air-dry weight for suspension aliquots in triplicate.

Depending on the experiment, the reddish-yellow, Fe-rich component, subsequently denoted herein as the 'middle' section, separated from the sediment comprising 9−17 wt.% of the initial sample (Table 2). Iron oxides were removed from selected samples of 'middle' section #1, using a citrate-dithionite-bicarbonate method (Mehra and Jackson, 1960), for further analysis. Samples of the middle section (both with and without Fe) were allowed to settle under gravity while air drying. The sedimented cakes were either ground gently in an agate mortar and pestle to obtain a uniform powder or left as 'oriented' cakes for further analysis by XRD.

Table 2. Approximate air-dried weight fractions of the TR soil separated for suspensions. The 2.5 and 5 wt.% samples did not remove all reddish-yellow components.

Sample	Wt.% top	Wt.% middle	Wt.% bottom
TRAD # 1 3−24 wt.%	0.2	17	82
TRAD # 2 2.5, 5.0 wt.%	–	9	91

The mineralogy was investigated using a combination of TGA and XRD. The TGA was performed using a HiRes TGA 2950 Thermogravimetric Analyzer, with helium as the purge gas. A high-resolution ramp (ramp 50ºC/min, 100−900ºC, equilibrate at 30ºC) option was set at a sensitivity level of five, where eight is the most sensitive level. This method varies the heating rate in response to changes in the rate of decomposition, resulting in improved weight-change resolution. Semi-quantitative analyses of the mineralogy were obtained using TGA. X-ray diffraction data were collected on a Bruker D8 X-ray Diffractometer by step scanning over the 2θ ranges of 3−70º with a step size of 0.02º and a dwell time of 5 s. Instrument parameters are listed in Table 3. The quartz in the sample was used as an internal standard to correct the data for any sample displacement error. Search-match identification of all the mineral phases was performed with Jade software (Version 6) from Materials Data Inc. Powder soil samples >2 μm in particle size were ground for 5 min in an agate mortar and pestle to reduce the average particle size to <2 μm. Ethanol was added as a lubricant to facilitate grinding and to minimize the alteration of heat-sensitive minerals. The ground powder and the remaining samples were packed into the 1" diameter, 1/16" deep well in a circular zero background quartz slide. The excess material on the

Table 3. XRD instrument parameters.

Radiation source	CuKα X-ray
Source power	45 kV, 40 mA
Wavelength	1.5405982 Å
Goniometer	Bruker D8
Divergence slit	1º
Divergence soller slit	None
Divergence antiscatter	1º
Specimen rotation	No
Diffracted beam antiscatter	1º
Diffracted beam soller Slit	2º
Secondary monochromator	Curved pyrolytic graphite
Receiving slit	0.15º
Detector	NaI scintillation
2θ range	3−70º
Step interval	0.02º(2θ)
Fixed counting time	5 s/step

surface was shaved off with a razor blade to reduce preferred orientation effects.

The BET surface area (SA) and associated measurements were obtained with a SA Micromeritics ASAP 2000. The adsorptive was N_2 at 77.35 K. Samples were degassed for 0.5 h at 30ºC at a pressure of 10 mm Hg. The adsorption leg of the isotherm was obtained using 60 points. Surface areas were calculated using the BET method (Brunauer *et al*., 1938) with 13 data points (p/p_o = 0−0.3) (Table 4) using the Micromeritics software.

The DT-1200 acoustic/electroacoustic spectrometer (Dispersion Technology) was used to obtain acoustic PSD and electroacoustic ζ potential measurements of various weight fractions of the TRAD suspensions, using a density of 2.65 g cm^{-3} for the solid. Densities for mineral standards were obtained from the DT-1200 software database (Dukhin and Goetz, 2002). Temperature, acoustic attenuation from 3−100 MHz, pH and CVI (Colloid Vibration Current) were recorded for each experiment. The sample was circulated with a peristaltic pump to assure a well mixed suspension, and suspensions were agitated with a Vortex Genie Mixer prior to analysis to assure a disaggregated sample. Acoustic/electroacoustic measurements were obtained in triplicate for 1.0 vol.% mineral standards (Table 4).

Experiments and analyses

The objective of the dilution experiment was twofold: to test the effects of dilution on PSD and ζ potential, and, to examine the effect of a large range of particle sizes on particle interactions. In this experiment, 170 mL of a 24 wt.% middle #1 suspension was diluted successively to 3 wt.% with AGW, and a series of analyses obtained at each weight fraction (Table 5, Figure 2).

The objective of the titration experiments was to determine the effect of pH on PSD and ζ potential at different suspension concentrations. Titrations were performed automatically using DT-1200 software on TRAD #2 suspensions at 2.5 (triplicate) and 5.0 (duplicate) wt.%, and on mineral standards for comparison. The 2.5 wt.% TRAD #2, gibbsite, kaolin, and goethite suspensions are all ~1.0 vol.%. Titration experiments were started near the 'natural' pH of each suspension in AGW: ~4.7 for TRAD; ~6.4 for gibbsite; ~5.5 for goethite; and ~5.3 for kaolinite. The pH was increased in regular steps to ~9.5 with 1.0 N NaOH, then decreased to ~4.0 with 1.0 N HCl. At each set point, acoustic attenuation and electroacoustic CVI measurements were obtained, as well as pH and temperature. Titrations took up to 2 h to complete.

Subsequent analysis of the attenuation spectra for PSD and the CVI measurement for ζ potential was accomplished using the DT-1200 software routines and associated theory (Dukhin and Goetz, 2001, 2002). The PSD is determined automatically by finding that distribution which provides the best fit between the predicted and measured attenuation spectra, considering the possibility of both a unimodal and a bimodal distributuion. When the fitting error for the bimodal distribution was ~2% lower than the lognormal, it was

Table 4. BET/N_2 surface area (SA), acoustic size (lognormal D(50)) and electroacoustic ζ potential of standards and selected TR sediment sections in AGW.

	BET SA (m^2 g^{-1})	Cumulative PoreVolume 1.7−300 nm (cm^3 g^{-1})	Size (μm)†	ζ potential. (mV)†	pH in AGW†
Goethite	33	0.13	0.9	55	5.5
Duke kaolin	17.3	0.1	0.1	−4.0	5.4
Gibbsite	6.1	0.03	0.9	42	6.4
Crushed Ottawa sand*	0.56	0.002	5.4	−65	6.6
TRAD sediment					
Middle #1**	27	0.08	Table 5	Table 5	Table 5
Middle #1 w/o Fe	15	0.06	n/m‡	n/m‡	n/m‡

* Heated to remove organic matter
** Average of four measurements.
† Average over triplicate measurements
‡ Not measured

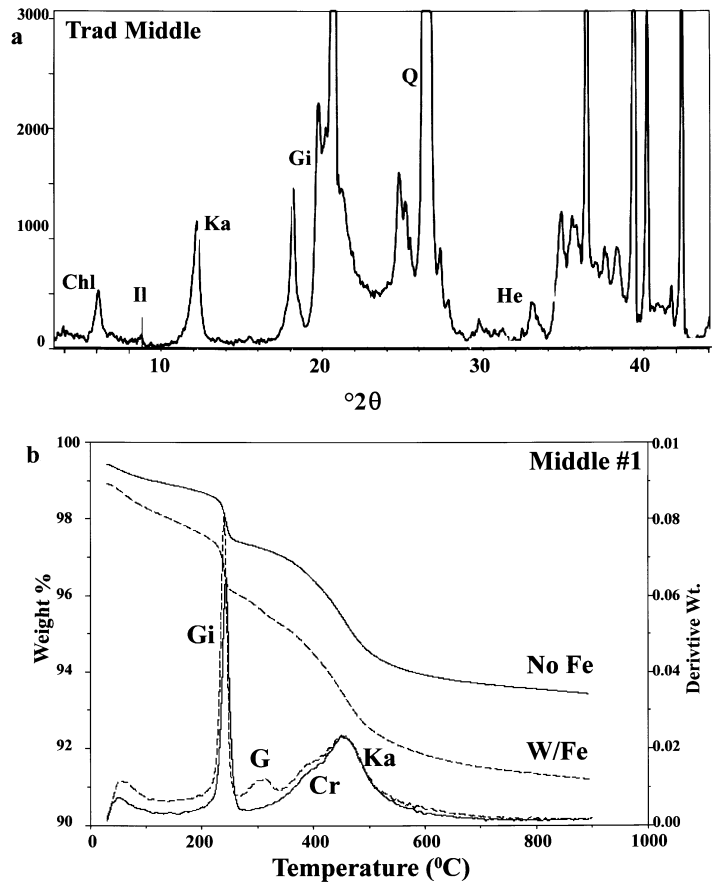

Figure 1. TRAD Middle #1 mineralogy. Gi – gibbsite, G – goethite/Fe oxides, Cr – crandallite, Ka – kaolinite, Chl – chlorite, Il – illite, Q – quartz, and He – hematite. (a) XRD pattern. (b) TGA analysis both with and without Fe oxides. The shoulder on the left side of the kaolin peak is crandallite (Cr).

selected as the preferred distribution (Dukhin and Goetz, 2002). The TRAD suspensions in most cases exhibited such bimodal distributions.

Following acoustic/electroacoustic analysis, selected suspensions were processed to obtain an independent measure of PSD (Table 7). One suspension (TRAD middle #1, 6 wt.%) was centrifuged unaltered, and produced no separation between the $\geqslant 2$ μm and <2 μm fractions. This sample, and all others, were then processed into <2 μm and $\geqslant 2$ μm fractions using a standard method of dispersion with NaOH followed by centrifugation (Jackson, 1979) with a Sorvall RC 5-B Plus centrifuge. For dispersion, 1 N NaOH was added to each of the sample bottles to obtain a pH of at least 8.5. The supernatant liquid was reddish in color, indicating that Fe-rich colloids remained in suspension even after centrifugation. The supernatant liquid was retained for further analysis by TGA. A 100 g sample of TR sediment was size fractionated by wet sieving (244 and 70 μm), the 70 μm fraction was split at 20 μm by settling and decantation (pH $\approx$9.5), and the 20 μm fraction was further split by centrifugation (Jackson, 1979). The results are listed in Table 1.

Table 5. Results from the dilution experiment on the 'middle' fraction of TRAD #1. See Figure 2. D(50) is the lognormal distribution size where 50 wt.% of the suspension is smaller/larger than this size. The error is the model fitting error for the distribution. The pH of all samples was 5.0–5.1.

	3 wt.%	6 wt.%	12 wt.%	24 wt.%
ζ potential (mV)	−3.6	−3.0	−2.3	−1.2
Lognormal				
D(50) (μm)	0.15	0.17	0.22	0.27
Fitting error (%)	7.3	7.5	9.3	8.4
Bimodal				
Mean small (μm)	0.14	0.17	0.21	0.27
Mean large (μm)	6.7	6	11.3	9.7
Fitting error (%)	5.8	5.4	6.5	5.4

RESULTS

Mineralogy, semi-quantitative mineral analysis and mineral characteristics

The mineralogy of the TRAD samples is reported in Table 1. Powder XRD patterns (Figure 1a) identified clays and clay minerals not identified via TGA. Analyses of similar sediments indicate the peak identified as chlorite may actually be hydroxy-interlayered

Table 6. TGA-estimated mineralogy for the TRAD sediment layers, averaged over ⩾3 analyses. The quartz fraction was calculated as the remaining wt.% after accounting for the other three minerals.

	% Gibbsite	% Goethite	% Kaolin	% Quartz[1]	Accounted Wt. loss[2]
TRAD #1 3–24 wt.%					
Top	11	16	38	35	82%
Top w/o Fe	11	–	35	54	77%
Middle #1	5	7	18	70	83%
Mid w/o Fe	4	–	18	78	75%
Bottom	–	–	–	100	–
TRAD #2 2.5, 5.0 wt.%					
Middle #2	10	10	30	50	83%
<2 μm disp'd	10	10	40	40	85–90%
⩾2 μm disp'd[4]	0–10	–	10	90	40–50%
Supernatant 2.5[5]	8	23	53	10	90%
Supernatant 5.0[5]	15	24	51	6	94%

Peak/total % loss for Standards	Gibbsite	Goethite	Duke Kaolin	Crush Ottawa[3]
	27.1/35.1	9.6/11.3	12.6/14.1	0.2/0.2

[1] By subtraction from estimated weight fraction
[2] Loss without accounting for quartz
[3] Ottawa Sand was heated to remove organic matter
[4] Dispersed with NaOH and centrifuged; >2 μm samples had very small weight loss, so values are uncertain
[5] Supernatant liquid from centrifuged TRAD dispersions at ~pH 9.0

vermiculite (Seaman *et al*., 1995a, 1995b). As some minerals (*e.g*. gibbsite, kaolin, goethite) have preferential orientations that alter dominant reflections (Brindley and Brown, 1984), XRD patterns for middle section 'oriented' cakes were obtained, and compared with kaolin and gibbsite 'cake' standards (not shown). The XRD patterns of TRAD cakes and TGA analyses (not shown) both show that the smallest size fraction is relatively enriched in kaolin.

Analyses by TGA (Table 6) of TRAD samples identified gibbsite, Fe oxides (probably goethite), kaolin and crandallite (shoulder on kaolin). Figure 1b shows TGA weight loss for TRAD #1 'middle' overlain by a sample with Fe oxides removed. Semi-quantitative analyses used a general TGA peak analysis scheme (Jackson, 1979) relating weight loss in mineral standards to loss in the corresponding sample peaks (Table 6). Prediction accuracy is ~10% (overestimate) in physical mixtures of kaolin and goethite. By subtracting the kaolin standard, the kaolin integration range was established by excluding some kaolin weight loss, and including some crandallite loss. Crandallite weight loss was ignored due to lack of a standard. Weight fractions were added using the following formula to find the percent sample loss attributed to the three minerals. In TRAD samples, ~75–90% of the total loss was accounted for:

$$\text{Accounted loss} = \frac{\left(\sum_{\text{mineral peaks}} \frac{\text{wt. loss for sample peak}}{\text{wt. loss for standard peak/total loss for mineral standard}} \right) 100}{\text{Total \% loss for sample}}$$

Analyses by TGA indicate that Fe oxide/goethite, gibbsite and kaolin are associated with the ⩽2 μm fraction as expected, and that crandallite is not associated with the smallest size fraction (supernatant liquid). The supernatant liquid of a dispersed 5 wt.% suspension is preferentially enriched in gibbsite, compared to a 2.5 wt.% suspension, although the mineralogy was initially the same (verified by TGA, not shown). A reddish color was observed in the dispersion supernatant liquid after centrifugation, and the color of the fractions remaining after dispersion changed. The color of the ⩾2 μm size fraction was pinkish white (Munsell® Soil Color Chart values: 7.5YR8/2) to white (Munsell® values: 10YR8/2). The color of the <2 μm size fraction was pink (Munsell® value: 7.5YR7/4) for all samples. The color of TRAD middle samples, unfractionated, was reddish yellow (Munsell® value: 7.5YR6/6).

The BET surface area analyses (Table 4) of the middle #1 section with and without Fe oxides indicate that about half of the BET surface area is due to the presence of Fe oxides. Given the low surface area of gibbsite, the remaining surface area is probably due mainly to kaolin. Acoustic PS and electroacoustic ζ potential from triplicate measurements are given in Table 4. Measurements given are within expected values (Hunter, 2001; Kosmulski, 2002).

Acoustic/Electroacoustic dilution experiment

A 'middle' TRAD #1 suspension was progressively diluted with AGW in three steps (24, 12, 6, 3 wt.%). The resulting acoustic attenuation spectra are regular, reproducible, and best fit with a bimodal distribution (Table 5), (Figure 2a). The lognormal D(50) (the particle size dividing the suspension into equal fractions by weight) and the small mode of the bimodal distribution were similar in size and decreased with suspension dilution. There was a corresponding increase in the absolute value of the ζ potential with dilution (Figure 2b).

These results indicate that some disaggregation occurred as the sediment/solution ratio decreased. The increased surface area exposed to the solution is evidenced by an increase in the CVI signal, and thus the change in the calculated ζ potential. The inclusion of large particles, possibly up to 70 μm, had little or no effect on the measured ζ potential. The PSD and ζ potential are obtained from (nearly) independent measurements (attenuation and CVI, respectively), so there is a high degree of confidence that the measured effect is real. The theoretical interpretation of the CVI signal requires an *a priori* size for the suspension. The calculated ζ potential is relatively insensitive to order of magnitude changes in the *a priori* size, resulting in a shift of only ~1 mV.

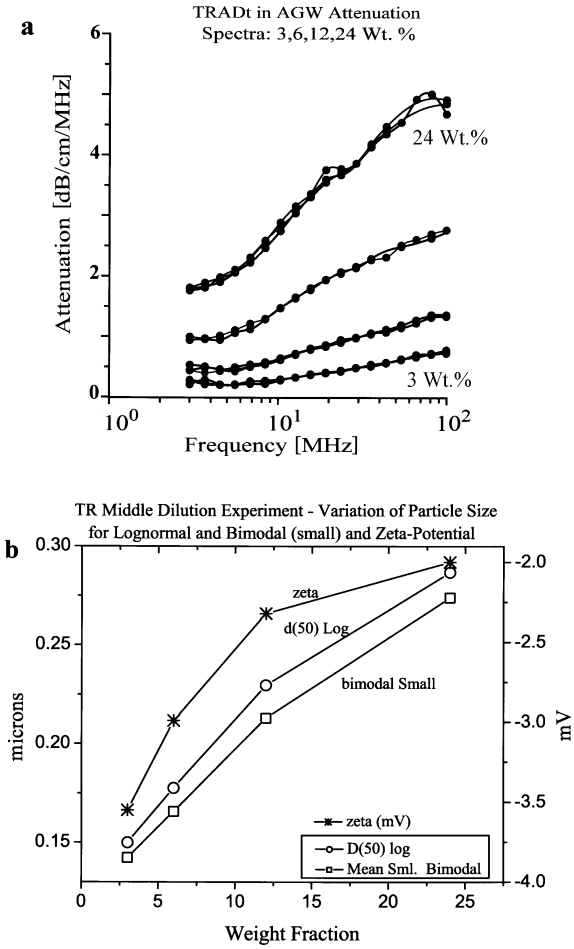

Figure 2. TRAD middle #1 dilution experiment results. The suspension pH was ~5.0–5.1. (a) Acoustic attenuation spectra (replicates shown) for suspensions at the four weight fractions. (b) Variation in particle size and ζ potential for the dilution experiment (see Table 6). As suspension concentration (soil/solution wt. fraction) decreased, ζ potential (mV) increased in absolute value and particle size for both lognormal D(50) and bimodal (small mode) decreased.

The size of the larger mode, which changes by a factor of ~2, is not related to changes in suspension concentration, PSD or ζ potential. This is probably due to difficulties in obtaining a uniform distribution of the largest particles during dilution. This observation verifies that the dilution process did not preferentially fractionate the smallest particles in the suspension, as changes in D(50) and CVI were regular with dilution, unlike the size of the larger mode. Concentrations of cations and anions in solution (not shown) increased slightly with suspension concentration, but not enough to shift the ζ potential.

Acoustic/electroacoustic pH titrations

During pH titrations on 2.5 wt.% suspensions (Figure 3), a large increase in the calculated size of both modes of the bimodal PSD was observed as the pH rose above pH ~7.5 and the ζ potential reached ~−12 mV. Triplicate titrations all exhibited a clear plateau in ζ potential from pH ~7.5 to 9.5, the maximum pH set point (Figure 3a). The plateau was not observed as pH decreased (Figure 3b). The attenuation spectra changed character at the onset of the plateau, indicating that aggregation had occurred (Figure 6a). The calculated changes in PSD were stable with time, and nearly irreversible with a decrease in pH (Figure 3b,d). Quartz/sand has a large negative ζ potential at the range of pH values used in these titrations (see Crushed Ottawa values, in Table 4, and 'Dispersion split' values, in Table 7), so it would not have influenced the appearance of a 'plateau'.

The observed changes in the attenuation and CVI that occurred during these titrations, which are independent of any theoretical model, indicate a 'real' effect, which was reproducible and independent of titration time (1 to >2 h). The most likely cause for the plateau and suspension instability is that the Fe and Al oxides reach a critical pH of ~7.5, in terms of their associations with the other minerals in the TRAD suspension. Recall, TRAD suspension supernatant liquid became reddish at high pH during dispersion by NaOH, and TGA analysis verified that Fe and Al oxides preferentially moved into the supernatant liquid (<0.2 μm fraction). The missing plateau at decreasing titration pH indicates the altered mineral associations were not re-established. Selected PSD results are detailed in Table 7.

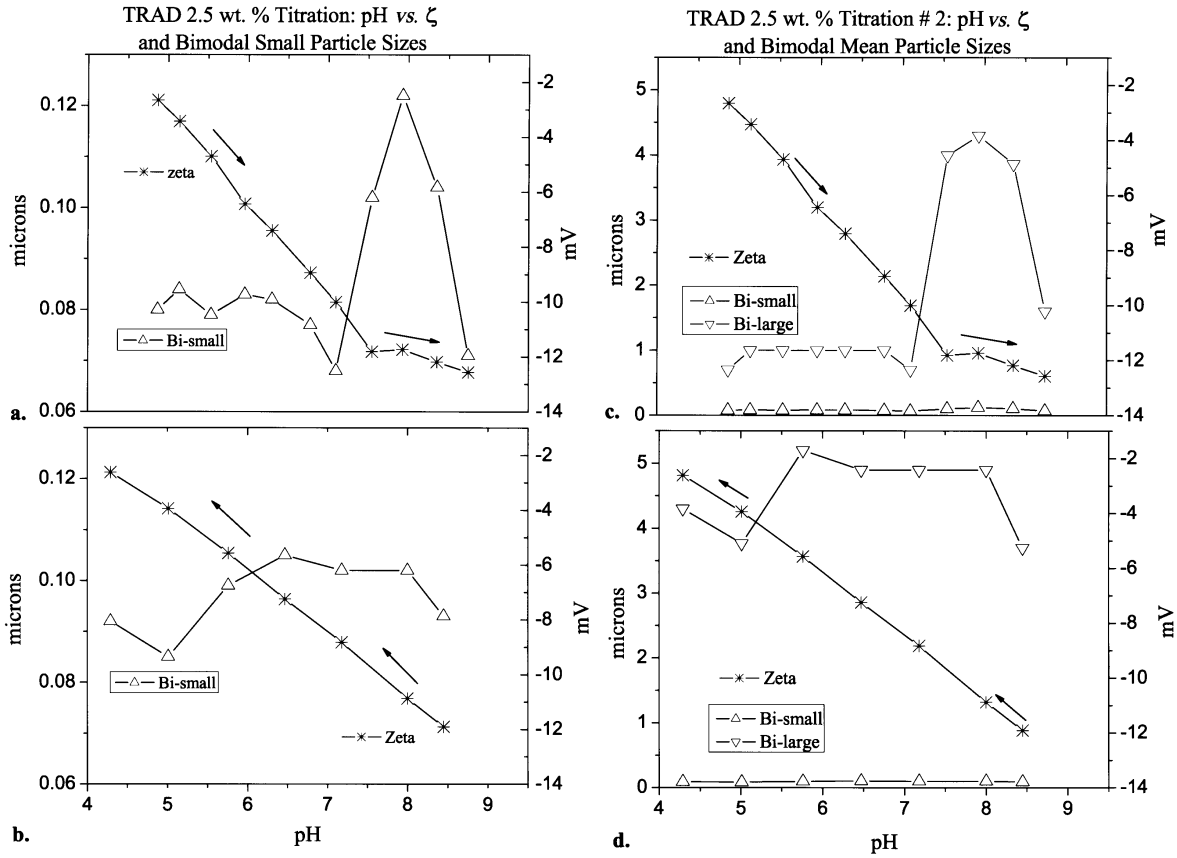

Figure 3. Titration of 2.5 wt.% TRAD #2 suspension, showing the variation in ζ potential and particle size for small (a,b) and large (c,d) modes of the bimodal distribution fit to the attenuation spectra. Fitting errors ranged from <4% to <7% for the bimodal fit. Arrows indicate titration progression. There was a time lapse of ~20 min between successive legs of the titration, which are plotted separately for clarity. (a,c) NaOH leg of titration. (b,d) HCl leg of titration.

In the 5 wt.% TRAD titrations, PSD results were relatively stable for both bimodal and lognormal fits at all pH values. There were only small variations in the attenuation spectra (Figure 6b), and the ζ potential did not plateau (Figure 4). In one titration (not shown), a small shift to larger bimodal sizes was observed near pH ≈7.5–8.0 (Table 7).

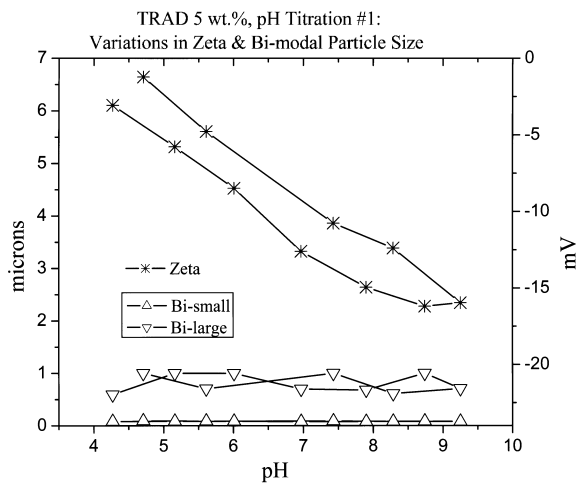

Figure 4. Titration of 5.0 wt.% TRAD #2 suspension. Arrows indicate titration progress. Results show the variation in ζ potential and particle sizes of the bimodal distribution fit at each indicated pH. Fitting errors ranged from <4% to <7%.

Kaolin, goethite and gibbsite titration results are shown in Figure 5. As the AGW is very dilute and the system is dominated by oxide minerals, the isoelectric point (IEP, the pH at which the electrophoretic mobility is zero) and the point of zero charge (pzc, the pH at which the electroacoustic ζ potential is zero) (Sposito, 1984, 1989) are nearly equal (Davis and Kent, 1990), the titration IEPs were compared with literature values for mineral pzc values for the purposes of this paper. The IEP was not reached for gibbsite (Figure 5a), but is probably pH ≈9.5. The IEP is pH ≈8.5 for goethite, and pH ≈4.5 for kaolinite (Figure 5b,c). Reported values for the pzc of goethite/ferrihydrite are in the range pH 7.2–10, depending on analysis technique, and for gibbsite the pzc is pH ≈8.0 or higher (Kosmulski, 2002). The kaolin suspension was stable throughout the titration (Figure 5f). The gibbsite and goethite attenuation spectra (Figure 5d,e, respectively) changed character at pH

Table 7. Comparison of PSD for the two sizing techniques. Acoustic PSD wt.% and ζ potential calculated with the DT-1200 software. The 'Dispersion split'[2] sample is the ⩾2 μm fraction of a TRAD Middle #1 sample, using dispersion and centrifugation. Selected analyses from the 2.5 and 5 wt.% titrations (Figures 3 and 4, respectively) are included.

	Acoustic PSD[1]		Dispersion/centrifuge	
	<2 μm (wt.%)	⩾2 μm (wt.%)	<2 μm (wt.%)	⩾2 μm (wt.%)
Dispersion split[2]	5%	95%	–	100%
Log mean	–	6.1 μm	–	–
ζ	–	−63 mV	–	–
pH	–	9.2	–	9.2
2.5 wt.%				
Low pH	100%	–	37%	63%
Mean-bimodal	0.08 μm, 0.7 μm	–	–	–
ζ	−3 mV	–	–	–
pH	4.7	–	>8.5	>8.5
High pH	70%	30%	–	–
Mean-bimodal	0.1 μm	3.7 μm	–	–
ζ	−12 mV	–	–	–
pH	8.4	–	–	–
5 wt.%				
Low pH	80%	20%	38%	62%
Mean-bimodal	0.1 μm, 1.0 μm	–	–	–
ζ	−2 mV	–	–	–
pH	4.7	–	>8.5	>8.5
High pH[3]	55%	45%		
Mean-bimodal	0.1 μm	3.1 μm	–	–
ζ	−18 mV	–	–	–
pH	9.2	–	–	–

[1] Wt.% values in acoustic measurements determined using DT-1200 software cumulative distributions
[2] Analysis of a 6 wt.% sample that was dispersed and centrifuged, and the >2 μm portion reanalyzed acoustically. ζ is large in value as Fe and Al oxide minerals are absent
[3] Titration results not shown

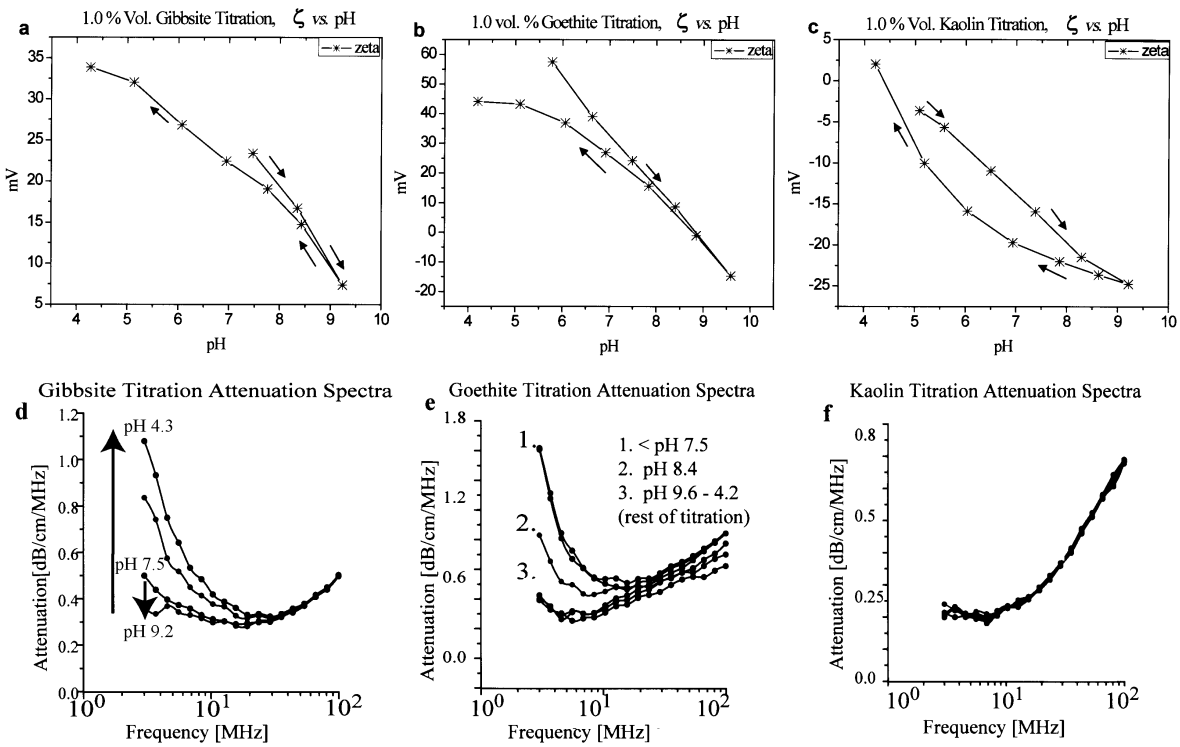

Figure 5. Titrations of the three 1.0 vol.% mineral standards in AGW, showing variation in ζ potential (a–c) and attenuation (d–f) during the titration. Arrows indicate titration progress. (a,d) Gibbsite titration. (b,e) Goethite titration. (c,f) Kaolinite titration.

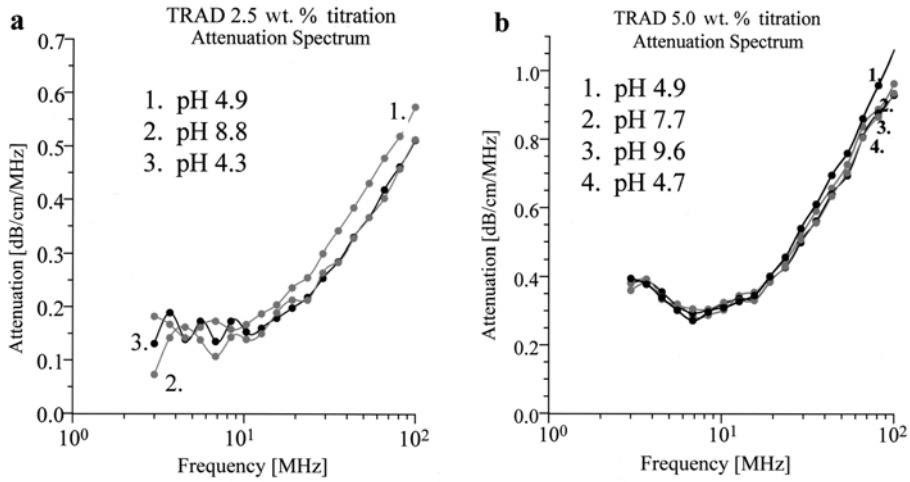

Figure 6. Variation in selected acoustic attenuation spectra during TRAD #2 titrations. Numbering indicates titration progress. (a) Variation in attenuation in 2.5 wt.% titration. The changes in low-frequency attenuation with pH are indicative of Al and Fe oxide minerals (compare with Figure 5d and e, respectively). (b) Variation in attenuation in 5.0 wt.% TRAD suspension is very small, and resembles the stability in the kaolinite titration (compare with Figure 5f).

$\approx$7.5, indicating that both of these suspensions became unstable as the ζ potential fell below ~20–25 mV. The change in character of the goethite attenuation spectra was not reversible with pH (Figure 5e), with attenuation remaining low at low frequencies as pH decreased. The gibbsite attenuation spectra behaved differently, with attenuation increasing at low frequencies as suspension pH decreased (Figure 5d).

The 'shape' of the TRAD ζ potential *vs*. pH curves (Figures 3, 4) is most similar to the kaolin titration curve (Figure 5c). Changes in the attenuation spectra during destabilization of the 2.5 wt.% sample at increasing pH incorporate aspects of the gibbsite and goethite attenuation spectra (Figure 5d,e), with attenuation decreasing at the lower frequencies (Figure 6a). As the suspension pH increases, the attenuation spectra appear to be a complex combination of the three mineral standards. At 5.0 wt.% (Figure 6b), the titration attenuation spectra appear most like kaolin (Figure 5f).

Particle sizing by dispersion/centrifugation

The results of particle sizing using dispersion/centrifugation are listed in Tables 1 and 7. There is a huge disparity between the acoustic results, which generally indicate a minority of $\geqslant$2 μm sized particles, and the dispersion/centrifugation results which indicate a majority of each suspension was $\geqslant$2 μm. Although the TRAD #1 and #2 suspensions incorporated very different weight fractions of the entire sediment (Tables 1 and 2), the dispersion PS results were very similar for each (not shown). A relevant observation is that the 2.5 wt.% TRAD acoustic PSD shifted to larger sizes at high pH (>7.5) during titrations (Figure 3), and dispersions were set at ~pH 9.0, or greater. The D(50) size for a dispersed and acoustically reanalyzed $\geqslant$2 μm sample ('Dispersion split', Table 7) was similar to the large bimodal size for the 'whole' suspension at high pH. A possible source of error in a calculated TRAD acoustic bimodal PSD is that the modeled distribution assumes the same standard deviation for each mode. However, this may not explain such a large disparity in PSD.

DISCUSSION

An underlying motivation of the research presented here is the attempt to understand how clays and clay minerals interact with each other, and with larger particles, in the sediment. Acoustic and electroacoustic analyses were used to investigate particle interactions in environmentally relevant suspension concentrations as a proxy of how they may interact in the field, and sample preparation was designed to minimize disruption. The mineralogy of the sediment suspensions is fairly complex, as is the interpretation of results for suspension concentration and pH titration effects. However, several important observations were made. Suspension concentration affected the PSD and ζ potential in the dilution experiment, and lower suspension concentrations were less stable during pH titrations. Titration results demonstrate the ability of acoustics/electroacoustics to measure *in situ* surface charge-related effects in both stable and unstable suspensions.

The dilution experiment resulted in a shift in PSD, so changes in ζ potential were due to a change in exposed surface area. Other authors (Hong and Xiao-Nian, 1992) found that variability in ζ potential (via electrophoretic mobility measurements) in different size fractions (<1.0 μm *vs*. 1–5 μm) depended on the mineralogy of the size fractions, particularly the Fe and Al oxide contents. Titration results herein showed that suspension stability is also dependent on suspension concentration. The Fe and Al oxide minerals apparently dominated

suspension stability and PSD at lower suspension concentrations. Theoretically, when inter-particle distance becomes less than the particle radius, this distance becomes a critical parameter, while particle radius is more important in dilute suspensions (Dukhin and Goetz, 2002). Inter-particle distance may have influenced the stability between the Fe and Al oxide and clay minerals in the 5.0 wt.% suspension more than in the 2.5 wt.% suspension. As both suspensions are quite dilute, it is not clear if either of these parameters is important here.

Some studies have shown that the addition of synthetic oxides of Al and Fe to kaolinite favors aggregation, significantly increasing the PSD (Arias *et al*., 1995). Amorphous Al precipitates were the most effective aggregant. Some researchers have suggested (Swartz *et al*., 1997) that an amorphous opal phase acts to bind colloidal particles in a sediment, in conjunction with Fe-mineral phases. In the current study, Al and Fe oxide minerals apparently control suspension stability. Differing dissolution/precipitation rates of these minerals may have affected titration kinetics, influenced by differences in suspension concentration and thus in solution composition. It is possible that the formation of Al, and possibly Fe, polymers at high pH in the TRAD suspensions influenced the measured aggregation. The TGA analyses of suspension supernatant liquid show gibbsite wt.% doubled with suspension concentration, although the initial mineralogy was the same in each suspension. This suggests that precipitation of an Al hydroxide mineral in the supernatant liquid (<0.2 μm, <1.0 wt.% of middle #2) at high pH may have increased suspension stability at the higher suspension concentration.

In general, suspensions become unstable when the ζ potential falls below 30 mV in absolute value (Dukhin and Goetz, 2002). In the TRAD suspensions, instability instead occurs near −12 mV, at a plateau in ζ potential. In investigating the effect of Fe^{3+} ions (from $FeCl_3$) on kaolin suspension ζ potential (via electrophoretic mobility), Ma and Pierre (1997) similarly found that flocculation sedimentation (characterized by a sharp interface between sediment and supernatant liquid in the suspension) occurred with $|\zeta|$ <10 mV, and accumulation sedimentation (under gravity) occurred with $|\zeta|$ >15 mV. Although the charge (*i.e*. the ζ potential) of the oxide phases, <15−25 mV in absolute value at high pH (Figure 5), appears to actually control TRAD suspension stability, this charge is 'masked' in the suspensions. Bulk suspension charge is thus a poor 'theoretical' indicator of mineralogical controls on suspension stability in such complex mixtures.

The biggest problem in utilizing acoustic attenuation spectra for obtaining a PSD is when the suspension contains both very small and very large particles (Dukhin and Goetz, 1996a, 1996b, 1998, 2002). This is the case with the TRAD suspensions. If we place confidence in acoustic titration results, we could conclude that the standard dispersion/centrifugation results are highly biased to large particle sizes due to aggregation in the suspensions at high pH, as initial low pH centrifugation experiments produced no separation at 2 μm. Alternatively, given the large range of particle sizes in these suspensions, it is likely that the largest particles were not included in the bimodal fits to the TRAD attenuation spectra, despite the great sensitivity of the acoustic technique (Dukhin and Goetz, 2002). In addition, the acoustic results indicating TRAD aggregation at high pH are somewhat counter-intuitive, so must be viewed with some skepticism. Thus, it is likely that both measures of PSD are biased – acoustics to smaller particle sizes, and dispersion/centrifugation to larger particle sizes. The PSD of these suspensions is perhaps best thought of as operationally defined.

CONCLUSIONS

The results presented in this paper have implications for the understanding of field and laboratory observations of colloid transport mechanisms. Different soil/solution ratios in soil pores may 'see' perturbations in solution ionic strength or pH differently. Perturbations such as these can induce both colloid mobilization and deposition (Bertsch and Seaman, 1999; Ryan and Elimelech, 1996; Ryan and Gschwend, 1994a, 1994b; Seaman and Bertsch, 2000). The acoustic and electroacoustic measurements provide *in situ* information on the effects of suspension concentration and pH on particle interactions in suspensions of highly weathered clays and clay minerals. Since attenuation measurements are independent of the electrical properties of the particle surfaces, they supply information about PSD that is independent of particle charge (Dukhin and Goetz, 2000), lending credibility to the combined acoustic/electroacoustic observations.

The mean particle size of the TR mineral suspensions decreased with suspension concentration in an artificial groundwater solution, resulting in an increase in the absolute value of the ζ potential. During pH titrations, suspension stability was also dependent on suspension concentration, with the higher concentration suspension more stable, at least over the duration of the titration. At lower suspension concentrations, the separate effects of kaolin and the Fe and Al oxide minerals were more easily distinguished. The effects of kaolin dominated the charge characteristics at low pH, while Fe and Al oxides dominated the charge characteristics, and thus suspension stability, at higher pH. Kinetic effects may explain some differences in titration results with suspension concentration. Future work will explore this possibility, as well as pursuing a more quantitative approach to interpreting TRAD attenuation and ζ potential (Dukhin and Goetz, 2002).

Acoustic/electroacoustic measurements indicate that aggregation occurred in the more dilute suspensions at high pH. Measurements of PSD, aggregation phenomena

and ζ potential, made *in situ*, raised doubts about the accuracy of results from the dispersion/centrifugation techniques, and we conclude that several methods are needed to understand particle-size distributions of complicated suspensions such as the ones we examined. The acoustic PSD results presented here are most likely skewed to smaller particle sizes, especially in suspensions with a greater range in particle sizes. Acoustic sizing analyses were very fast, taking <10 min, and CVI measurements took a few minutes. Although CVI measurements can be made with sample volumes of a few mL, a limiting factor in experiments was that large sample volumes (>150 mL) were required for combined acoustic/electroacoustic work The more common sizing technique of fractionation via chemical dispersion and centrifugation provided important supplementary information, but was time consuming, and the sizing results are suspect due to chemical effects induced by the 'dispersion' process.

ACKNOWLEDGMENTS

This research was supported by the DOE Center for Excellence in Water Research and partially by Financial Assistance Award Number DE-FC09-96SR18546 from the DOE to The University of Georgia Research Foundation. The authors thank Paul Maddox, Derek Harmon and Angel Kelsey-Wall for their assistance in technical aspects of sample preparation and analysis.

REFERENCES

Anderson, B.R. and Benjamin, M.M. (1990) Surface and bulk characteristics of binary oxide suspensions. *Environmental Science and Technology*, **24**, 692–698.

Arias, M., Barral, M.T. and Diaz-Fierros, F. (1995) Effects of iron and aluminum oxides on the colloidal and surface properties of kaolin. *Clays and Clay Minerals*, **43**, 406–416.

Bertsch, P. and Seaman, J. (1999) Characterization of complex mineral assemblages: Implications for contaminant transport and remediation. *Proceedings of the National Academies of Science, USA*, **96**(March), 3350–3357.

Brindley, G.W. and Brown, G. (1984) *Crystal Structures of Clay Minerals and their X-ray Identification*. Monograph **5**, Mineralogical Society, London, 495 pp.

Brunauer, S., Emmett, P.H. and Teller, E. (1938) Adsorption of gases in multimolecular layers. *Journal of the American Chemical Society*, **60**, 309–319.

Bunn, R.A. (2002) Mobilization of natural colloids from an iron oxide coated sand aquifer: effect of pH and ionic strength. *Environmental Science and Technology*, **36**, 314–322.

Cerpa, A., García-González, M.T., Tartaj, P., Requena, J., Garcell, L. and Serna, C.J. (1999) Mineral content and particle-size effects on the colloidal properties of concentrated lateritic suspensions. *Clays and Clay Minerals*, **47**, 515–521.

Costa, A.L., Galassi, C. and Greenwood, R. (1999) Alpha-alumina-H_2O interface analysis by electroacoustic measurements. *Journal of Colloid and Interface Science*, **212**, 350–356.

Davis, J.A. and Kent, D.B. (1990) Surface complexation modeling in aqueous geochemistry. Pp. 177–260 in: *Mineral-Water Interface Geochemistry* (A.F. White, editor). Reviews in Mineralogy, **23**. Mineralogical Society of America, Washington, D.C.

Dukhin, A.S. and Goetz, P.J. (1996a) Acoustic and electroacoustic spectroscopy. *Langmuir*, **12**, 4336–4344.

Dukhin, A.S. and Goetz, P.J. (1996b) Acoustic spectroscopy for concentrated polydisperse colloids with high density contrast. *Langmuir*, **12**, 4987–4997.

Dukhin, A.S. and Goetz, P.J. (1998) Characterization of aggregation phenomena by means of acoustic and electroacoustic spectroscopy. *Colloids and Surfaces*, **144**, 49–58.

Dukhin, A.S. and Goetz, P.J. (2000) Characterization of concentrated dispersions with several dispersed phases by means of acoustic spectroscopy. *Langmuir*, **16**, 7597–7604.

Dukhin, A.S. and Goetz, P.J. (2001) *Installation Handbook and User Manual – Model DT-1200 Electroacoustic Spectrometer*. Dispersion Technology, Bedford Hills, New York, USA.

Dukhin, A.S. and Goetz, P.J. (2002) *Ultrasound for Characterizing Colloids*. Studies in Interface Science, **15**. Elsevier, Amsterdam, 372 pp.

Dukhin, A.S., Ohshima, H., Shilov, V.N. and Goetz, P.J. (1999a) Electroacoustics for concentrated dispersions. *Langmuir*, **15**, 3445–3451.

Dukhin, A.S., Shilov, V.N., Ohshima, H. and Goetz, P.J. (1999b) Electroacoustic phenomena in concentrated dispersions: New theory and CVI experiment. *Langmuir*, **15**, 6692–6706.

Dukhin, A.S., Goetz, P.J. and Truesdail, S. (2001) Titration of concentrated dispersions using electroacoustic potential probe. *Langmuir*, **17**, 964–968.

Galassi, C., Costa, A.L. and Pozzi, P. (2001) Influence of ionic environment and pH on the electrokinetic properties of ball clays. *Clays and Clay Minerals*, **49**, 263–269.

Guerin, M. and Seaman, J.C. (2004) Characterizing clay mineral suspensions using acoustic and electroacoustic spectroscopy – a review. *Clays and Clay Minerals*, **52**, 145–157.

Honeyman, B.D. (1984) Cation and anion adsorption at the oxide/solution interface in systems containing binary mixtures of adsorbents: an investigation of the concept of adsorptive additivity. PhD thesis, Stanford University, Stanford, 383 pp.

Hong, Z. and Xiao-Nian, Z. (1992) Contribution of iron and aluminum oxides to electrokinetic charge characteristics of variable charge soils in relation to surface charge. *Pedosphere*, **2**, 31–42.

Hunter, R.J. (1981) *Zeta Potential in Colloid Science*. Academic Press, New York.

Hunter, R.J. (1998) Recent development in the electroacoustic characterization of colloidal suspensions and emulsions. *Colloids and Surfaces*, **141**, 37–65.

Hunter, R.J. (2001) *Foundations of Colloid Science*. Oxford University Press, New York.

Hunter, R.J. and James, M. (1992) Charge reversal of kaolinite by hydrolyzable metal ions: An electroacoustic study. *Clays and Clay Minerals*, **40**, 644–649.

Jackson, M.L. (1979) *Soil Chemical Analysis: Advanced Course*. M.L. Jackson, Madison, Wisconsin, USA.

Johnson, S.B., Russell, A.S. and Scales, P.J. (1998) Volume fraction effects in shear rheology and electroacoustic studies of concentrated alumina and kaolin suspensions. *Colloids and Surfaces*, **141**, 119–130.

Johnson, S.B., Dixon, D.R. and Scales, P.J. (1999a) The electrokinetic and shear yield stress properties of kaolinite in the presence of aluminum ions. *Colloids and Surfaces*, **146**, 281–291.

Johnson, S.B., Scales, P.J. and Healy, T.W. (1999b) The binding of monovalent electrolyte ions on alpha-alumina. 1. Electroacoustic studies at high electrolyte concentrations. *Langmuir*, **15**, 2836–2843.

Kosmulski, M. (2002) The pH-dependent surface charging and points of zero charge. *Journal of Colloid and Interface Science*, **235**, 77–87.

Ma, K. and Pierre, A.C. (1997) Effect of interaction between clay particles and Fe^{3+} ions on colloidal properties of kaolinite suspensions. *Clays and Clay Minerals*, **45**, 733–744.

McClements, D.J. (1991) Ultrasonic characterisation of emulsions and suspensions. *Advances in Colloid and Interface Science*, **37**, 33–72.

Mehra, O.P. and Jackson, M.L. (1960) Iron oxide removal from soils and clays by a diothionite-citrate system buffered with sodium bicarbonate. *Proceedings of the Seventh International Clay Conference*. Earth Science, Pergamon Press, New York.

O'Brien, R.W., Cannon, D.W. and Rowlands, W.N. (1995) Electroacoustic determination of particle size and zeta potential. *Journal of Colloid and Interface Science*, **173**, 406–418.

Rowlands, W.N. and Hunter, R.J. (1992) Electroacoustic study of adsorption of cetylpryidinium chloride on kaolinite. *Clays and Clay Minerals*, **40**, 287–291.

Roy, W.R., Krapac, I., Chow, S.F.J. and Griffin, R.A. (1991) *Batch-type procedures for estimating soil adsorption of chemicals*. EPA/530-SW-87-006-F, US Environmental Protection Agency, Champaign, Illinois, USA.

Ryan, J.N. and Gschwend, P.M. (1994a) Effect of solution chemistry on clay colloid release from an iron oxide coated aquifer sand. *Environmental Science and Technology*, **28**, 1717–1726.

Ryan, J.N. and Gschwend, P.M. (1994b) Effects of ionic strength and flow rate on colloid release: Relating kinetics to intersurface potential energy. *Journal of Colloid and Interface Science*, **164**, 21–34.

Ryan, J.N. and Elimelech, M. (1996) Colloid mobilization and transport in groundwater. *Colloids and Surfaces, A: Physicochemical and Engineering Aspects*, **107**, 1–56.

Schwertmann, U. and Cornell, R.M. (1991) *Iron Oxides in the Laboratory: Preparation and Characterization*. VCH Publishers, Inc., New York.

Seaman, J.C. and Bertsch, P.M. (2000) Selective colloid mobilization through surface charge manipulation. *Environmental Science and Technology*, **34**, 3749–3755.

Seaman, J.C., Bertsch, P.M. and Miller, W.P. (1995a) Chemical controls on colloid generation and transport in a sandy aquifer. *Environmental Science and Technology*, **29**, 1808–1815.

Seaman, J.C., Bertsch, P.M. and Miller, W.P. (1995b) Ionic tracer movement through highly weathered sediments. *Journal of Contaminant Hydrology*, **20**, 127–143.

Seaman, J.C., Bertsch, P.M. and Strom, R.N. (1997) Characterization of colloids mobilized from Southeastern Coastal Plain Sediments. *Environmental Science and Technology*, **31**, 2782–2790.

Sindi, I., Biscan, J. and Pravdic, V. (1996) Electrokinetics of pure clay minerals revisited. *Journal of Colloid and Interface Science*, **178**, 514–522.

Sposito, G. (1984) *The Surface Chemistry of Soils*. Oxford University Press, New York, 234 pp.

Sposito, G. (1989) *The Chemistry of Soils*. Oxford University Press, New York, 277 pp.

Strom, R.N. and Kaback, D.S. (1992) *SRP Baseline Hydrogeologic Investigation: Aquifer Characterization Groundwater Geochemistry of the Savannah River Site and Vicinity (U)*. Westinghouse Savannah River Company, Environmental Sciences Section, USA, 98 pp.

Swartz, C.H., Ulery, A.L. and Gschwend, P.M. (1997) An AEM-TEM study of nanometer-scale mineral associations in an aquifer sand: Implications for colloid mobilization. *Geochimica et Cosmochimica Acta*, **61**, 707–718.

Yong, R.N. and Ohtsubo, M. (1987) Interparticle action and rheology of kaolinite-amorphous iron hydroxide (ferrihydrite) complexes. *Applied Clay Science*, **2**, 63–81.

(*Received 10 January 2003; revised 6 October 2003; Ms. 747*)